The impact of shipping, agricultural, and urban emissions on single particle chemistry observed aboard the R/V *Atlantis* during CalNex

Cassandra J. Gaston,[1,6] Patricia K. Quinn,[2] Timothy S. Bates,[2] Jessica B. Gilman,[3,4] Daniel M. Bon,[3,4,7] William C. Kuster,[3,4] and Kimberly A. Prather[1,5]

Received 23 October 2012; revised 12 April 2013; accepted 17 April 2013; published 28 May 2013.

[1] The Research at the Nexus of Air Quality and Climate Change (CalNex) field campaign was undertaken to obtain a better understanding of the regional impacts of different pollution sources in California. As part of this study, real-time shipboard measurements were made of the size-resolved, single-particle mixing state of submicron and supermicron particles (0.2–3.0 μm aerodynamic diameter) along the California coast where major differences were noted between Southern and Northern California. In Southern California, particles containing soot made up the largest fraction of submicron particles (~38% on average and up to ~89% by number), whereas organic carbon particles comprised the largest fraction of submicron number concentrations (~29% on average and up to ~78% by number) in Northern California including the Sacramento area. The mixing state of these carbonaceous particle types varied during the cruise with sulfate being more prevalent on soot-containing particles in Southern California due to the influence of fresh shipping and port emissions in addition to contributions from marine biogenic emissions. Contributions from secondary organic aerosol species, including amines, and nitrate were more prevalent in Northern California, as well as during time periods impacted by agricultural emissions (e.g., from the inland Riverside and Central Valley regions). These regional differences and changes in the mixing state and sources of particles have implications for heterogeneous reactivity, water uptake, and cloud-nucleating abilities for aerosols in California.

Citation: Gaston, C. J., P. K. Quinn, T. S. Bates, J. B. Gilman, D. M. Bon, W. C. Kuster, and K. A. Prather (2013), The impact of shipping, agricultural, and urban emissions on single particle chemistry observed aboard the R/V *Atlantis* during CalNex, *J. Geophys. Res. Atmos.*, *118*, 5003–5017, doi:10.1002/jgrd.50427.

1. Introduction

[2] Atmospheric aerosols contribute to air pollution, have adverse effects on human health, and perturb the Earth's radiative balance [*Poschl*, 2005]; both aerosol size and composition play key yet uncertain roles in these effects. One aim of the Research at the Nexus of Air Quality and Climate Change (CalNex) field campaign was to elucidate the links between aerosols, air pollution, and climate in order to guide policies regarding emission regulations in California. Diverse particle sources impact California including ships, vehicle exhaust, oil refineries, meat cooking, and animal husbandry and agricultural emissions. The Ports of Los Angeles (LA) and Long Beach (LB) are the busiest container ports in the United States, contributing high levels of ship and port emissions (e.g., diesel truck emissions, oil refinery emissions) to Southern California. Locations in inland Southern California (e.g., Riverside) and the Sacramento and San Joaquin Valley areas in Northern California are impacted by dairy farm and agricultural emissions leading to high mass concentrations of particulate matter that contain large fractions of secondary species [*Chen et al.*, 2007; *Chow et al.*, 2006a; *Docherty et al.*, 2008; *Grover et al.*, 2008; *Hughes et al.*, 2000, 2002; *Magliano et al.*, 1999; *Pastor et al.*, 2003; *Qin et al.*, 2012; *Sorooshian et al.*, 2008]. Furthermore, biogenic emissions from forested regions such as the Sierra Nevada foothills and from marine biological activity along the California coast also contribute to the aerosol burden in California [*Creamean et al.*, 2011; *Gaston et al.*, 2010]. Assessing how these regional differences in

[1]Scripps Institution of Oceanography, University of California, San Diego, La Jolla, California, USA.
[2]NOAA Pacific Marine Environmental Laboratory, Seattle, Washington, USA.
[3]NOAA Earth System Research Laboratory, Boulder, Colorado, USA.
[4]Cooperative Institute for Research in Environmental Sciences (CIRES), University of Colorado Boulder, Boulder, Colorado, USA.
[5]Department of Chemistry and Biochemistry, University of California, San Diego, La Jolla, California, USA.
[6]Now at Department of Atmospheric Sciences, University of Washington, Seattle, Washington, USA.
[7]Now at Planning and Policy Program, Air Pollution Control Division, Colorado Department of Public Health and Environment, Denver, Colorado, USA.

Corresponding author: K. A. Prather, Department of Chemistry and Biochemistry, University of California, San Diego, La Jolla, CA 92093-0314, USA. (kprather@ucsd.edu)

2169-897X/13/10.1002/jgrd.50427

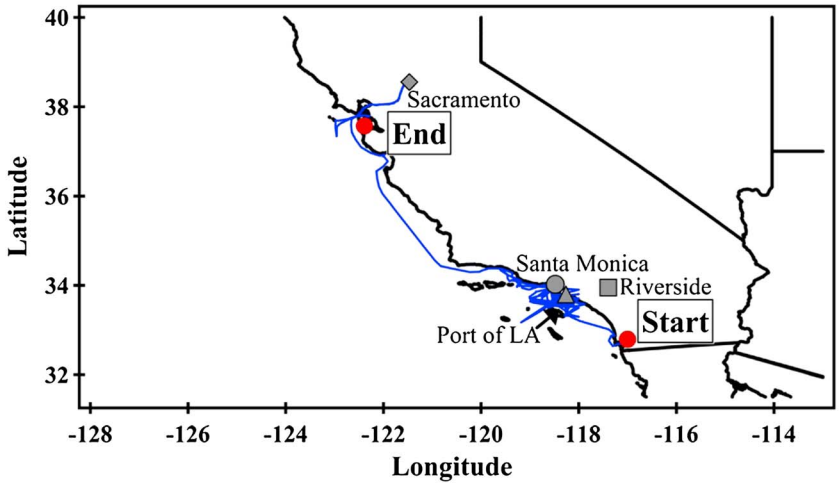

Figure 1. Cruise track for the R/V *Atlantis* (blue line) along the California coast during CalNex. The Port of Los Angeles (grey triangle), the Santa Monica area (grey dot), Riverside (grey square), and the Sacramento area (grey diamond) are shown along with the start and end points of the cruise.

particle sources and secondary reactions in California impact the physicochemical properties of aerosols represents a key step in fulfilling the goals of the CalNex field campaign.

[3] Single-particle mass spectrometry is well suited for providing the high temporal resolution and mass spectral fingerprints necessary for distinguishing diverse particle sources and assessing the impact of atmospheric processing (e.g., gas-to-particle partitioning, heterogeneous reactions, etc.) on particle size and chemistry [*Pratt and Prather*, 2011; *Sullivan and Prather*, 2005]. Aerosol time-of-flight mass spectrometry (ATOFMS), a single-particle technique, has been successfully used for the source apportionment of particulate matter in California for almost 15 years [*Ault et al*., 2010; *Creamean et al*., 2011; *Gaston et al*., 2010; *Hughes et al*., 2000; *Moffet et al*., 2008b; *Noble and Prather*, 1996; *Pastor et al*., 2003; *Pratt et al*., 2009; *Pratt and Prather*, 2009; *Qin et al*., 2012; *Toner et al*., 2008; *Whiteaker et al*., 2002]. Herein we present real-time measurements of single-particle composition and size using ATOFMS during the CalNex campaign onboard the R/V *Atlantis* sampling platform. Atmospheric measurements were made off the California coast, targeting specific sources, including the Ports of LA and LB, continental outflow from the LA Basin, and emissions from Northern California including the inland Sacramento area. This paper describes the significant differences observed in single-particle mixing state and sources between these regions. The implications of these findings are discussed.

2. Experiment

2.1. CalNex

[4] Ambient aerosol and gas-phase measurements were made onboard the R/V *Atlantis* from 14 May to 8 June 2010 as part of the CalNex 2010 field campaign [*Ryerson et al*., 2013; http://www.esrl.noaa.gov/csd/calnex/; http://saga.pmel.noaa.gov/data]. The ship traveled from San Diego to Sacramento and then back to the Port of San Francisco where the study ended. The cruise track is shown in Figure 1. The air in the aerosol sampling manifold was conditioned to $60 \pm 5\%$ relative humidity (RH) using a heated inlet. Insulated conductive tubing extending from the heated inlet provided air to the instruments at flows of ~30 Lpm [*Bates et al*., 2004]. Meteorological parameters, aerosol properties, and gas-phase constituents such as radon, SO_2, O_3, etc., were measured onboard the ship [*Quinn and Bates*, 2005]. Hydrocarbons, including toluene and benzene, were quantified using gas chromatography equipped with a flame ionization detector [*Bon et al*., 2011]. The ratio of toluene to benzene can be used as an indicator of photochemical age [*Gelencser et al*., 1997; *Roberts et al*., 1984]. Air masses containing fresh urban emissions that have undergone minimal photochemical processing typically have toluene/benzene ratios ≥2; lower values are indicative of more photochemically processed air masses as the more reactive toluene is preferentially removed by reactions with the hydroxyl radical. Clean marine air masses are typically well aged and are expected to have toluene/benzene ratios ≪1. Ship exhaust from the R/V *Atlantis* was filtered out by eliminating time periods when the relative wind direction was aft of +100° (starboard) and −120° (port) off the bow. All data presented here were filtered using this method. Data are presented in coordinated universal time (UTC), which is 7 h ahead of local time (PDT), as day of year (DOY). For example, a date and time of 12:00 on 1 January presented in UTC would correspond to DOY 1.5.

2.2. Aerosol Measurements: ATOFMS

[5] The size-resolved chemical composition of individual aerosol particles from 0.2 to 3.0 μm aerodynamic diameter was measured in real time using aerosol time-of-flight mass spectrometry (ATOFMS). The operating principles of the ATOFMS have been described previously [*Gard et al*., 1997; *Prather et al*., 1994]. Briefly, particles are sampled through a converging nozzle inlet into a differentially pumped vacuum chamber causing particles to be accelerated to a size-dependent terminal velocity. Particles next enter the sizing region of the instrument consisting of two continuous

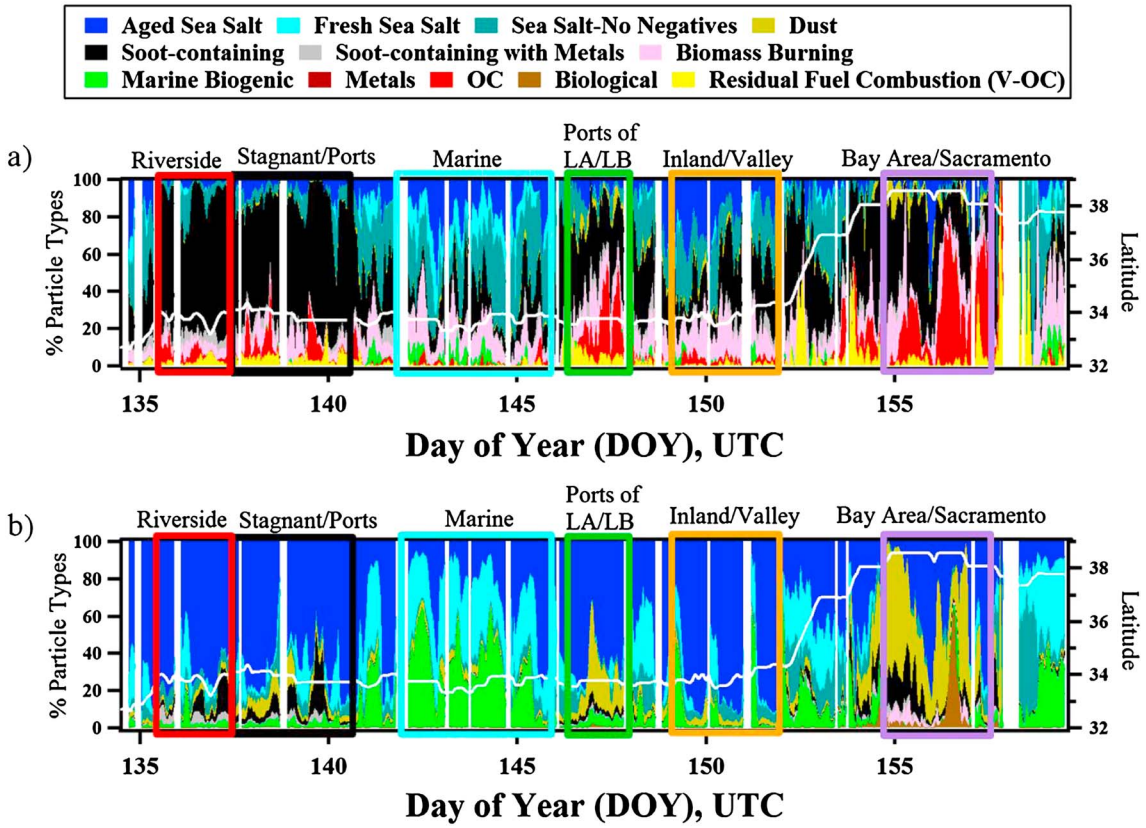

Figure 2. Hourly temporal profile of single-particle mixing-state observed by ATOFMS in UTC as a function of day of year (DOY) and latitude (white line). Single-particle chemistry for (a) submicron particles (0.2–1.0 μm) and (b) supermicron particles (1.0–3.0 μm), respectively. Colored boxes highlight six different periods when differences in particle composition were observed due to different meteorological conditions, gas-phase concentrations, and aging processes.

wave (532 nm) lasers separated by a fixed distance. The time taken to traverse the laser beams is recorded giving the terminal velocity of the particle, which is used to calculate the aerodynamic diameter of the particle. The particle velocity is also used to time the firing of a Q-switched neodymium:yttrium/aluminum/garnet laser (266 nm) operating at ~1.2 mJ laser power that simultaneously desorbs and ionizes compounds from individual particles creating positive and negative ions, which are analyzed in a dual polarity time-of-flight mass spectrometer. Particle detection efficiencies are dependent on the ability of particles to interact with the 266 nm radiation [*Dall'Osto et al.*, 2006; *Qin et al.*, 2006; *Wenzel et al.*, 2003]. Dual-polarity spectra provide complementary information regarding the source (e.g., ships versus sea salt) and age of the particle (e.g., fresh versus reacted sea salt) [*Guazzotti et al.*, 2001; *Noble and Prather*, 1996]. A lack of negative ion spectra indicates the presence of tightly bound particle phase water, which suppresses negative ions produced by laser desorption/ionization [*Neubauer et al.*, 1997, 1998]. Conditioning particles to 60% RH decreases some of this water, thus increasing the formation of negative ion spectra.

[6] The YAADA software toolkit was used to import ion peak lists into MATLAB v 6.5.1 (The MathWorks, Inc.) for processing of ATOFMS data [*Allen*, 2002]. Single-particle mass spectra were then analyzed using a clustering algorithm (ART-2a), which groups spectra together with similar characteristics into distinct "clusters" [*Song et al.*, 1999]. These "clusters" are then merged into distinct particle types based on the prevalent mass spectral ions and intensities, which are indicative of particle sources and chemistry [*Noble and Prather*, 1996]. The prevalence of these particle types was averaged into 1 h time bins and separated into submicron (0.2–1.0 μm) and supermicron (1.0–3.0 μm) particles. Each ion peak assignment presented in this paper corresponds to the most likely ion produced at a given mass-to-charge (*m/z*). Particle types described herein are defined by characteristic ion peaks and/or possible sources and do not reflect all of the species present within a particular particle class.

3. Results

[7] Temporal trends of single-particle measurements were analyzed to discern differences in particle composition between sources in Southern and Northern California. The temporal variability of the most frequently observed particle types detected by ATOFMS as well as the latitudinal position of the ship is shown in Figures 2a and 2b for submicron and supermicron particles, respectively. Several trends in single-particle mixing state were identified based on differences in particle source, meteorological conditions, and aging processes. To illustrate this, six distinct time periods are identified by colored boxes in Figure 2; the time periods are

Table 1. Meteorological and Gas Phase Data for Six Different Air Mass Transport Conditions[a]

Period	Location/Air Mass	Day of Year (DOY)	Date and Time (UTC)	Latitude	Longitude	Wind Speed (m/s)	RH (%)	Air Temp (°C)	Radon (mBq/m^3)	SO_2 (ppbv)	Ozone (ppbv)	Toluene/ Benzene
1	Riverside	135.5–137.375	5/15/2010 12:00 to 5/17/2010 9:00	33.14°N to 34.02°N	118.33°W to 119.22°W	2.93	89	13.2	2500	0.07	47.1	N/A
2	Stagnant/Ports	137.375–140.5	5/17/2010 9:00 to 5/20/2010 12:00	33.67°N to 34.38°N	118.22°W to 119.69°W	3.86	91	13.4	1060	0.06	39.0	0.40
3	Marine/Coastal	142–146	5/22/2010 0:00 to 5/26/2010 0:00	33.31°N to 33.95°N	118.07°W to 118.93°W	5.18	72	13.9	1550	0.14	35.1	0.85
4	Ports of LA/LB	146.33–147.875	5/26/2010 8:00 to 5/27/2010 21:00	33.53°N to 33.77°N	118.1°W to 118.5°W	2.40	73	16.0	740	3.40	29.3	1.89
5	Inland/Valley	149–151.875	5/29/2010 0:00 to 5/31/2010 21:00	33.5°N to 34.4°N	118.17°W to 119.85°W	3.29	83	15.2	3200	0.45	43.6	0.84
6	Bay Area/ Sacramento	154.625–157.625	6/3/2010 15:00 to 6/6/2010 15:00	38.02°N to 38.56°N	121.55°W to 122.16°W	4.53	69	20.9	1550	0.42	22.8	1.74

[a]Day of year (DOY), date and time (UTC), latitudinal and longitudinal range, average meteorological conditions (wind speed, RH, air temperature), and average gas-phase concentrations (radon, SO_2, ozone, and the toluene/benzene ratio) for measurements made during each of the six different time periods are highlighted. Dates are formatted as month/day/year.

defined as Riverside Transport (Period 1, boxed in red), Stagnant/Ports Transport (Period 2, boxed in black), Marine/Coastal Transport (Period 3, boxed in cyan), Ports of Los Angeles/Long Beach (LA/LB) (Period 4, boxed in green), Inland/Valley Transport (Period 5, boxed in orange), and Bay Area/Sacramento (Period 6, boxed in purple). The following sections provide a detailed comparison and discussion of the gas-phase species and meteorological conditions, prevalent particle types and sources, the mixing state of carbonaceous particles, and the secondary particulate species present during each time period.

3.1. Characteristics of Each Period

[8] During the Riverside, Stagnant/Ports, and Marine/Coastal Transport periods, measurements took place along the Southern California coast focusing on emissions from the LA Basin, whereas measurements during the Ports of LA/LB period were entirely performed in the Ports of LA and LB and surrounding shipping lanes. During the Inland/Valley Transport period, measurements extended farther north to include the Santa Barbara region; the Bay Area/Sacramento period measurements were made in Northern California when the ship remained in the Deep Water Channel/Sacramento region for 3 days. Table 1 shows the corresponding dates and meteorological and gas phase measurements for each time period. Figure 3 shows the 48 h calculated air mass back trajectories at 500 m height [*Draxler and Rolph*, 2011] for each time period to highlight differences in air mass transport conditions. The Stagnant/Ports and Ports of LA/LB periods were heavily influenced by emissions from the Ports of LA/LB while the Riverside, Stagnant/Ports, Inland/Valley, and Bay Area/Sacramento periods were influenced by agricultural and urban emissions from Riverside and/or the Central Valley. The Marine/Coastal Transport period was influenced by oceanic emissions and serves as a background period.

3.1.1. Period 1: Riverside Transport

[9] During the Riverside Transport period, Hybrid Single-Particle Lagrangian Integrated Trajectory analysis indicates that the sampled air masses were transported from the Riverside and Imperial Valley regions before traversing the port and Santa Monica regions (see Figure 3a). Thus, the Riverside Transport period is expected to be influenced by urban, port, and agricultural emissions. Particulate matter in Riverside typically is well aged as indicated by high concentrations of secondary species such as nitrate, amines, ammonium, and secondary organics [*Hughes et al*., 2000; 2002; *Liu et al*., 2000; *Pastor et al*., 2003; *Pratt et al*., 2009; *Pratt and Prather*, 2009; *Qin et al*., 2012]. The ratio of toluene to benzene was not available during this period; however, available NO_x/NO_y ratios indicated that the air masses during this period were photochemically aged. The average radon concentration was high (2500 ± 760 mBq/m^3) indicating that continentally influenced air masses were sampled. The average temperature was low (13.2 ± 0.6°C) while RH was high (89 ± 3%).

3.1.2. Period 2: Stagnant/Ports Transport

[10] Sampled air masses stagnated around the coast near the ports and Santa Monica region during the Stagnant/Ports Transport period. Thus, port emissions (e.g., emissions from vehicles, ships, etc.) contributed more significantly to the aerosol burden during the Stagnant/Ports Transport than the Riverside Transport period. Some air masses also

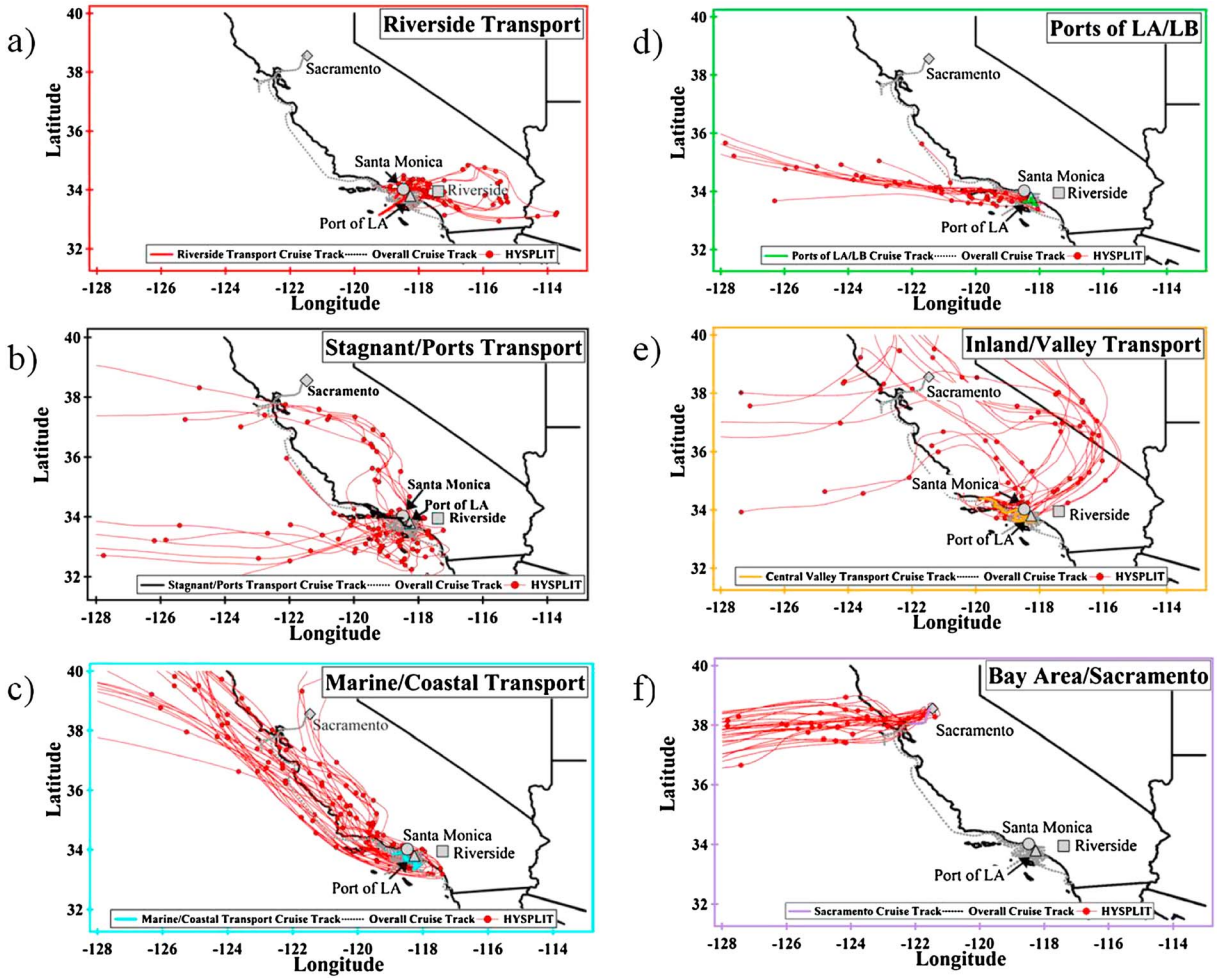

Figure 3. The 48 h Hybrid Single-Particle Lagrangian Integrated Trajectory air mass back trajectories at 500 m (red lines) shown during the cruise (grey dotted line) corresponding to (a) Period 1: Riverside Transport boxed in red, (b) Period 2: Stagnant/Ports Transport boxed in black, (c) Period 3: Marine/Coastal Transport boxed in cyan, (d) Period 4: Ports of LA/LB boxed in green, (e) Period 5: Inland/Valley Transport boxed in orange, and (f) Period 6: Bay Area/Sacramento boxed in purple. Red dots on the HYSPLIT trajectories denote 12 h increments. The Port of Los Angeles (grey triangle), the Santa Monica area (grey dot), Riverside (grey square), and the Sacramento area (grey diamond) are also shown.

originated from the inland Central Valley area toward the end of the Stagnant/Ports Transport period potentially carrying agricultural emissions. The lowest average toluene to benzene ratio, 0.4, was observed during this period suggesting that air masses sampled during this period were heavily photochemically aged. Again, high RH ($91 \pm 3\%$ on average) and low temperatures ($13.4 \pm 1.1°C$) were observed.

3.1.3. Period 3: Marine/Coastal Transport

[11] During the Marine/Coastal Transport period, most air masses followed a northern coastal/oceanic trajectory along the California coast. Wind speeds reached 14.5 m/s, which enhanced the production of fresh sea spray particles from bursting bubbles generated by breaking waves [*Blanchard and Woodcock*, 1957; *Monahan et al.*, 1983; *O'Dowd and De Leeuw*, 2007]. Thus, the Marine/Coastal Transport period is characterized by ocean-derived aerosol composed of both fresh sea salt and biogenic organics. This period is not necessarily representative of clean marine conditions based on the relatively high radon concentrations (1550 ± 1080 mBq/m^3) and high average particle number counts (5721 ± 2680 cm^{-3}) [*Fitzgerald*, 1991; *Hawkins et al.*, 2010; *O'Dowd and De Leeuw*, 2007; *Twohy et al.*, 2005]. Further evidence that the Marine/Coastal Transport period is not entirely a clean marine period also stems from the toluene to benzene ratio, which ranged from 0.030 during clean marine conditions to 3.74 when fresh urban emissions were encountered with an average of 0.85.

3.1.4. Period 4: Ports of LA/LB

[12] The Ports of LA/LB period was characterized by high $SO_{2(g)}$ concentrations (3.4 ± 5.2 ppbv on average with a maximum of 40 ppbv) compared to the previous periods when average $SO_{2(g)}$ concentrations ranged from 0.06 to 0.45 ppbv. Furthermore, low wind speeds (2.4 ± 1.2 m/s) and low radon concentrations (740 ± 320 mBq/m^3) were also encountered. Toluene to benzene ratios were high with an average of 1.89 and a maximum of 6.1 indicating a photochemically unprocessed air mass. It is likely that local urban, port, and shipping emissions dominated the particle composition during this period with little influence from other continental or transported sources.

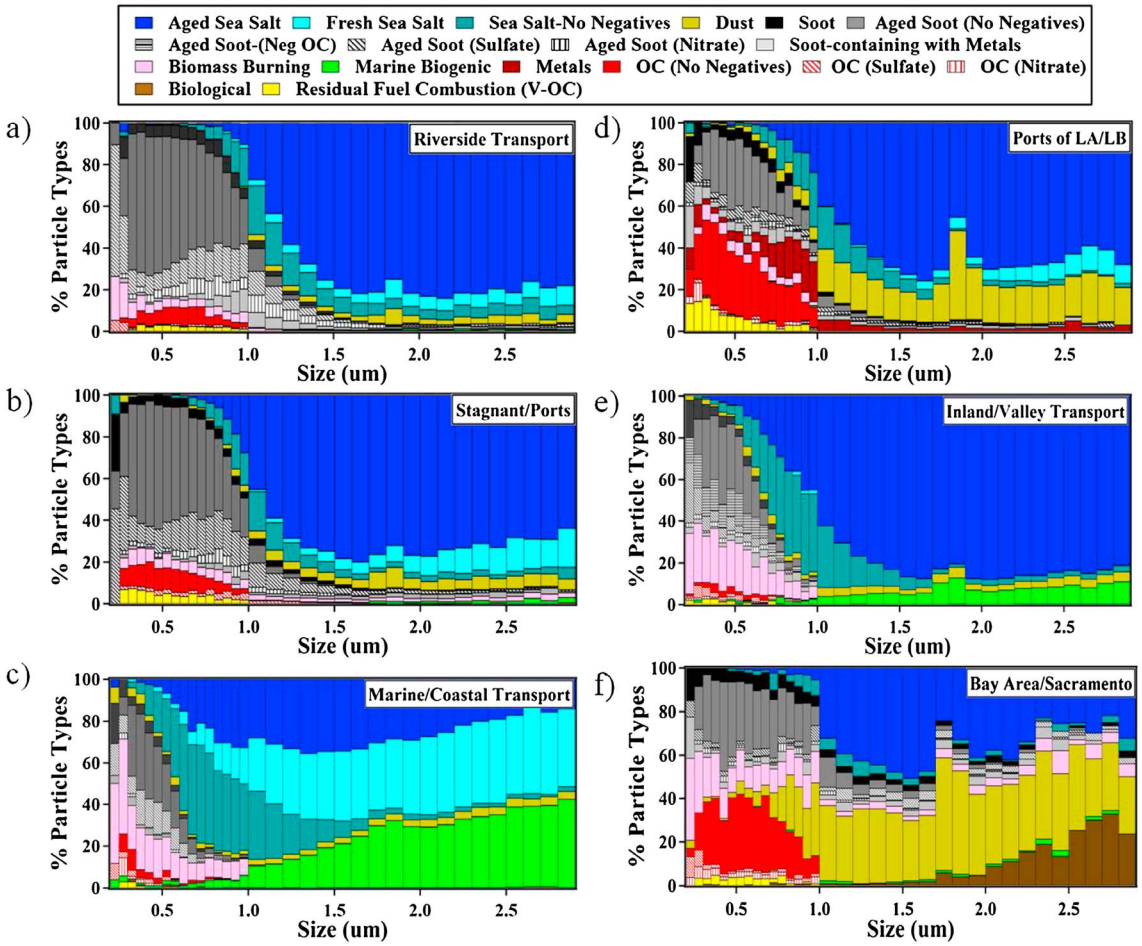

Figure 4. Fraction of particle types as a function of size observed during the six different time periods. Submicron particles (0.2–1.0 μm) are plotted in 0.05 μm bins while supermicron particles (1.0–3.0 μm) are plotted in 0.1 μm bins.

3.1.5. Period 5: Inland/Valley Transport

[13] Figure 3e shows air masses traveling across the Central Valley and the desert before traversing the LA Basin and Santa Barbara regions during the Inland/Valley Transport period. Higher radon and $O_{3(g)}$ concentrations were measured during this time period compared to other time periods with averages of 3200 ± 3000 mBq/m^3 and 44 ± 11 ppbv, respectively. Toluene to benzene ratios had an average of 0.84 indicating that air masses sampled during this period were fairly well aged. Similar to Riverside, aerosol from the Central Valley is typically characterized by high concentrations of secondary species, namely, secondary organic aerosol and ammonium nitrate due to contributions from dairy farms and other agricultural emissions in addition to urban emissions from sources such as vehicles [*Chen et al.*, 2007; *Chow et al.*, 2006a; 2006b; *Eatough et al.*, 2008]. Hence, particulate matter observed during this period is expected to show similar signs of particle aging as the Riverside Transport period.

3.1.6. Period 6: Bay Area/Sacramento

[14] During the Bay Area/Sacramento period, air masses traveled over the San Francisco Bay area prior to arriving in the Sacramento region, which is within the Central Valley. Diurnal temperature and RH profiles were observed with night and day values ranging from 16 to 30°C and 24 to 93%, respectively. High toluene to benzene ratios were observed with an average of 1.74, suggesting that the sampled air masses were relatively fresh, similar to the Ports of LA/LB period; however, unlike the Ports of LA/LB period, sampling during the Bay Area/Sacramento period occurred within the Central Valley and not within a major port region.

3.2. Observed Particle Types

3.2.1. Submicron Particle Composition

[15] Particle composition varied based on sources and transport conditions (Figures 2 and 4). High number fractions of soot-containing particles (up to ~89% of submicron particles by number with an average of ~38 ± 27%) were observed in Southern California, particularly during the Riverside Transport, Stagnant/Ports Transport, and Ports of LA/LB periods (Periods 1, 2, and 4) when port and urban (e.g., vehicles) emissions were dominant. The main exception to this trend in high soot-containing number fractions in Southern California occurred during the Marine/Coastal Transport period (Period 3) when submicron particle composition was dominated by sea-salt particles (~63 ± 17% of submicron particles on average) due to air mass transport conditions. The dominance of soot-containing particles in Southern California is in agreement with aircraft ATOFMS measurements made during CalNex where *Cahill et al.*

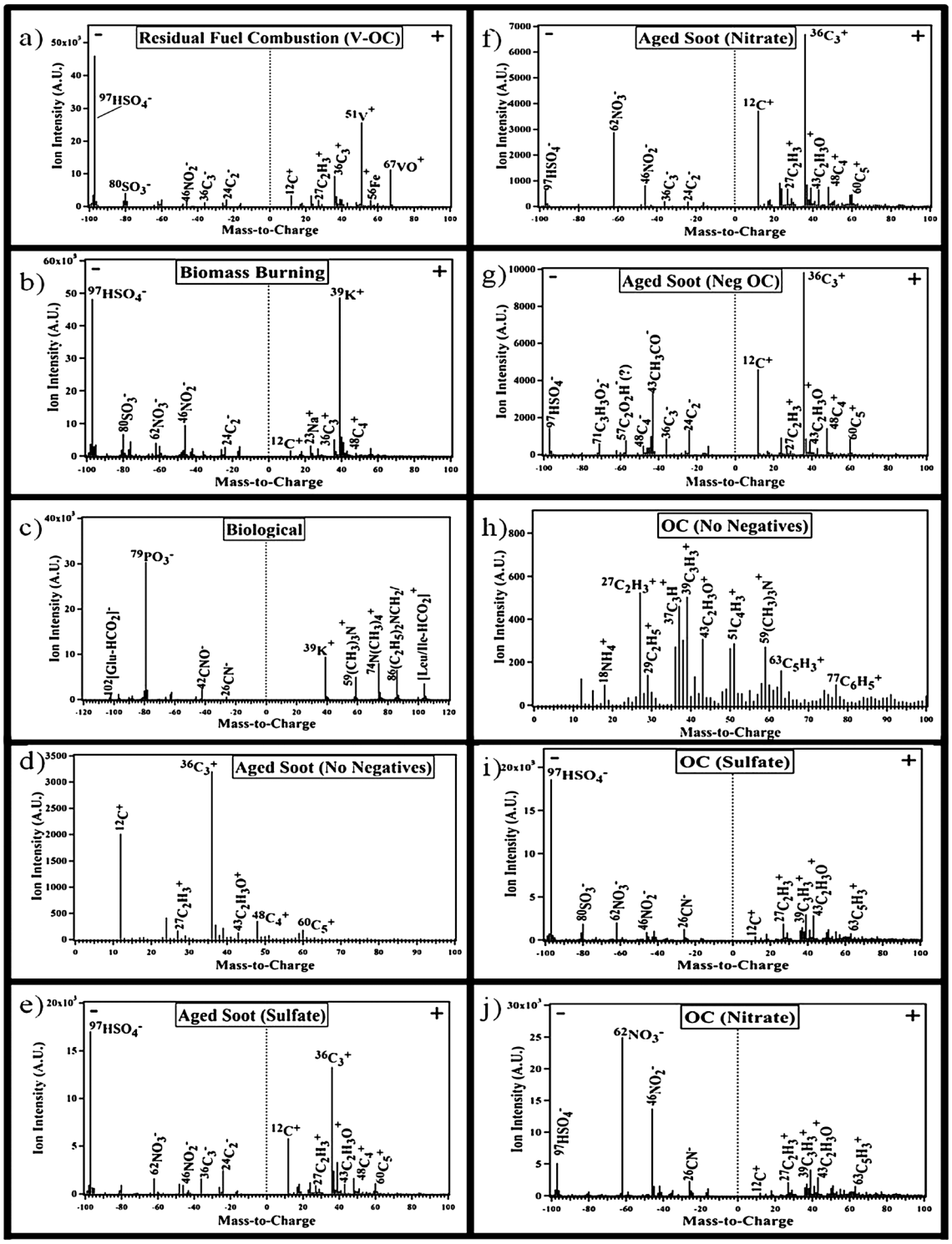

Figure 5. Representative mass spectra of (a) Residual Fuel Combustion from ships (V-OC), (b) Biomass Burning, (c) Biological, (d) Aged Soot (No Negatives), (e) Aged Soot (Sulfate), (f) Aged Soot (Nitrate), (g) Aged Soot (Neg OC), (h) OC (No Negatives), (i) OC (Sulfate), and (j) OC (Nitrate) particles are shown. For mass spectra containing both positive and negative ions, dashed lines separate negative ions (left side) and positive ions (right side).

[2012] reported high soot-containing number fractions in the Southern California/LA Basin region.

[16] In addition to the soot-containing particle type, particles from residual fuel combustion (e.g., emissions from ships and oil refineries) were also observed, namely, during the Stagnant/Ports Transport and Ports of LA/LB periods when port and shipping emissions heavily influenced particle composition. This residual fuel combustion particle

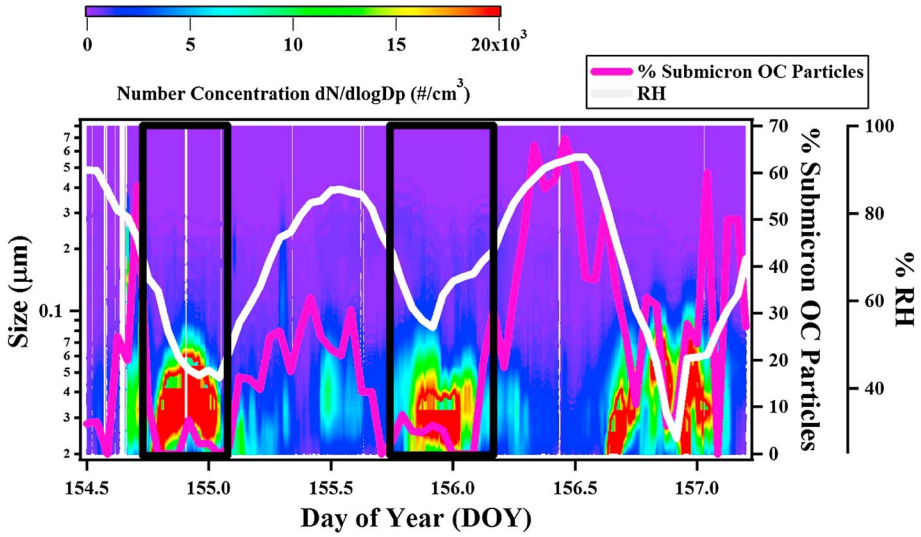

Figure 6. Size distributions of particle number concentrations as a function of size and DOY are shown on a log scale. The percentage of submicron OC particles detected by ATOFMS (pink line) and RH (grey line) are shown as a function of DOY. Time periods when new particle formation events were observed are shown in black boxes.

type represented at most ~25% of submicron particles and is characterized by ion peaks associated with transition metals found in residual fuel oil, notably vanadium ($^{51}V^+$, $^{67}VO^+$), nickel ($^{58,60}Ni^+$), and iron ($^{54,56}Fe^+$), in addition to organic carbon, sulfate ($^{97}HSO_4^-$) and, to a lesser extent, nitrate ($^{46}NO_2^-$, $^{62}NO_3^-$) (see Figure 5a for an example mass spectrum); these particles are herein referred to as vanadium-organic carbon (V-OC) particles [*Agrawal et al.*, 2008; *Ault et al.*, 2010; 2009; *Corbett and Fischbeck*, 1997; *Healy et al.*, 2009; *Murphy et al.*, 2009]. During the Ports of LA/LB period, additional industrial particle types were observed, including metals concentrated in the submicron size mode, which most likely represent emissions from incineration [*Moffet et al.*, 2008a] and are the subject of a different paper [*Weiss-Penzias et al.*, 2013]. Additionally, organic carbon (OC) represented a much higher fraction of the detected submicron particles during the Ports of LA/LB period (~14 ± 14% of the total submicron particles detected, on average) than previous periods likely due to elevated fossil fuel emissions in the Ports of LA and LB from vehicles, heavy-duty diesel trucks, and ships, which have been shown to contribute high mass concentrations of organic carbon to the aerosol burden [*Lack et al.*, 2009; *Murphy et al.*, 2009; *Russell et al.*, 2000; *Sodeman et al.*, 2005].

[17] In contrast, soot-containing and V-OC particles made smaller contributions to the number concentration in Southern California during Inland/Valley Transport conditions and in the Northern California, Sacramento region during the Bay Area/Sacramento period (Periods 5 and 6). As shown in Figures 2 and 4, particles from biomass burning were elevated in the submicron mode during these two periods representing up to ~61% of submicron particles. Biomass-burning particles are characterized by an intense potassium peak ($^{39}K^+$) in addition to carbonaceous peaks (both elemental and organic), organic nitrogen peaks ($^{26}CN^-$, $^{42}CNO^-$), ion peaks associated with potassium salts ($^{113}K_2Cl^+$, $^{213}K_3SO_4^+$, etc.), and secondary species such as sulfate and/or nitrate (Figure 5b) [*Pratt et al.*, 2010; *Qin and Prather*, 2006; *Silva et al.*, 1999].

[18] The key difference in particle composition observed in Northern California during the Bay Area/Sacramento period (Period 6) was the high percentage of submicron OC particles detected, constituting ~29 ± 23% of submicron particles by number on average and up to ~78%. Unlike the OC detected during the Ports of LA/LB period, which originated from fossil fuel sources in the Ports of LA and LB, OC detected in Sacramento is likely the result of biogenic emissions due to the fact that biogenics were dominant during the first half of the Carbonaceous Aerosol Radiative Effects Study (CARES) in the Sacramento Valley [*Cahill et al.*, 2012]. Numerous new particle formation (NPF) events were observed across the Sacramento Valley during CalNex and the first part of CARES during this period [*Ahlm et al.*, 2012; *Setyan et al.*, 2012]. While the lower size limit of the nozzle-inlet ATOFMS (~0.2 µm) cannot be used to probe the composition of newly formed particles, ATOFMS measurements can provide insight into the composition of these particles as they grow to sizes detectable by the instrument [*Creamean et al.*, 2011]. Figure 6 shows particle number concentration as a function of diameter measured by a differential mobility particle sizer [*Bates et al.*, 2012]. Two distinct events are highlighted in black boxes when high number concentrations of small particles (~0.02 µm) were observed followed by rapid growth, which is indicative of NPF events [*Creamean et al.*, 2011; *Hegg and Baker*, 2009; *Kulmala*, 2003]. As shown in Figure 6, the percentage of OC particles was smallest when the NPF event was actually occurring. This is because the size of the newly formed particles is below the size detection limit of the instrument. The percentage of OC particles increased primarily after these NPF events occurred as the newly formed particles grew to sizes detectable by the instrument suggesting that organics contributed to this growth in agreement with previous studies [*Creamean et al.*, 2011; *Kulmala*, 2003; *Smith et al.*, 2008; *Zhang et al.*, 2004], and with recent measurements during CARES in the Sacramento Valley from an aerosol mass spectrometer [*Setyan et al.*, 2012]. The formation of new

particles occurred under conditions of lower RH and intense solar radiation; these low RH conditions also favor the formation of high molecular weight secondary organic aerosol from biogenic emissions that may have contributed to particle formation and/or growth [*Nguyen et al*., 2011]. Growth of these particles into sizes detectable by the ATOFMS occurred as RH increased with many of the detected OC particles lacking negative ion spectra ($85 \pm 16\%$ on average) indicating that an appreciable amount of particulate water was associated with these particles [*Neubauer et al*., 1997; 1998].

3.2.2. Supermicron Particle Chemistry

[19] Aged sea salt dominated the supermicron particle composition during most periods making up $50 \pm 27\%$ of total supermicron particles on average, as shown in Figures 2 and 4. Aged sea-salt particles result from heterogeneous reactions with gas-phase nitrogen oxides (e.g., $N_2O_{5(g)}$, $HNO_{3(g)}$), which lead to the displacement of chloride and the formation of particulate nitrate [*Behnke et al*., 1991; *Chang et al*., 2011; *Gard et al*., 1998; *Vogt et al*., 1996]. In addition to nitrate, methanesulfonic acid (MSA) and sulfate were also found on ~14% of aged sea-salt particles, on average, possibly contributing to the observed particulate chloride displacement [*Hopkins et al*., 2008; *Laskin et al*., 2012]. During the Marine/Coastal Transport period (Period 3), fresh sea salt and marine biogenic particle types dominated the supermicron particle composition making up $33 \pm 11\%$ and $30 \pm 17\%$ of supermicron particles on average, respectively. Marine biogenic particle types include Mg-type [*Gaston et al*., 2011] and sulfur-type particles (C. J. Gaston et al., manuscript in preparation, 2013), which represent ocean-derived particle types associated with marine biological activity and/or dissolved organic material. The combined high wind speeds in addition to the elevated biological activity, as evidenced by the presence of red tide blooms along the Southern California coast (www.sccoos.org), explain the dominance of fresh sea salt and marine biogenic emissions during this period.

[20] Marine particle types were negligible in the inland Sacramento region during the Bay Area/Sacramento period. Instead, dust particles were found to represent $39 \pm 23\%$ of supermicron particles, and biological particles were found to constitute up to ~64% of supermicron particles as shown in Figures 2 and 4f. Most of the biological particles detected by ATOFMS were determined to be spores containing dipicolinic acid, a compound that is easily detected using laser/desorption ionization at 266 nm radiation and serves as a unique matrix allowing for the detection of amino acids, which typically have low absorption cross sections at 266 nm [*Silva and Prather*, 2000; *Srivastava et al*., 2005]. Consistent with previous measurements of spores using laser/desorption ionization at 266 nm, spores detected during CalNex contained $^{39}K^+$, $^{59}(CH_3)_3N^+$, $^{74}(CH_3)_4N^+$, *m/z* +86 due to either $(C_2H_5)_2NCH_2^+$ or the amino acids [leucine-HCO_2] and [isoleucine-HCO_2], *m/z* +104, which is yet to be identified, phosphate ($^{63}PO_2^-$, $^{79}PO_3^-$), organic nitrogen ($^{26}CN^-$, $^{42}CNO^-$), and *m/z* −123, which is most likely due to dipicolinic acid-HCO_2 (Figure 5c) [*Srivastava et al*., 2005]. Spores have rarely been detected by ATOFMS in ambient environments and represent a very unique particle type most likely detected due to agricultural and biogenic emissions from the Sacramento area.

3.3. Variations in the Mixing State of Carbonaceous Particle Types

3.3.1. Soot Particle Mixing State

[21] In addition to probing overall particle composition, observed differences in the mixing state of soot-dominated particles were also investigated (Figure 7a). These particles are characterized by intense elemental carbon ion peaks ($^{12}C^+$, $^{36}C_3^+$, $^{48}C_4^+$,…C_n^+). A small percentage of freshly emitted elemental carbon particles, herein referred to as "soot," contained intense elemental carbon peaks indicative of long-chain elemental carbon (e.g., elemental carbon ion peaks extending out to higher masses in both the positive and negative ion spectra) with only low-intensity peaks from secondary species such as sulfate and/or nitrate [*Cahill et al*., 2012; *Moffet and Prather*, 2009]. Most of the soot-containing particles, however, contained intense elemental carbon peaks that did not extend out to higher masses and were internally mixed with low-intensity organic peaks ($^{27}C_2H_3^+$, $^{43}C_2H_3O^+$, etc.) in addition to other secondary species (e.g., nitrate and/or sulfate) in agreement with aircraft observations during CalNex [*Cahill et al*., 2012; *Metcalf et al*., 2012]. This second class of soot-containing particles is herein referred to as Aged Soot particles, consistent with *Cahill et al*. [2012], and is further subdivided into Aged Soot (No Negatives), Aged Soot (Sulfate), Aged Soot (Nitrate), and Aged Soot (Neg OC) particle classes. Overall, the majority of Aged Soot particles (~$62 \pm 20\%$ of soot-containing particles on average) lacked negative ion spectra and are classified as Aged Soot (No Negatives) (see Figures 5d and 7a), with sizes peaking in number concentration at ~0.5–0.6 μm and extending up into the supermicron size range (Figure 4). The lack of negative ion spectra and larger sizes suggests that these particles contained appreciable particulate water [*Moffet et al*., 2008b; *Neubauer et al*., 1997; 1998] possibly due to cloud or fog processing.

[22] The most striking trend shown in Figure 7a is the high percentage of Aged Soot (sulfate) particles detected in Southern California (representing, on average, ~$30 \pm 18\%$ of detected submicron soot-containing particles during the Riverside Transport, Stagnant/Ports Transport, Marine/Coastal Transport, and Ports of LA/LB periods) that decreased significantly to ~$11 \pm 10\%$ as the ship moved north along the California coast. Aged Soot (sulfate) particles are characterized by intense sulfate peaks ($^{80}SO_3^-$, $^{97}HSO_4^-$; Figure 5e) [*Moffet and Prather*, 2009]. This trend in Aged Soot (sulfate) particles is in contrast to aircraft measurements made by ATOFMS, which mainly observed internal mixtures of soot and nitrate as opposed to sulfate in Southern California [*Cahill et al*., 2012] due to the accumulation of ammonium nitrate coatings [*Metcalf et al*., 2012]. The most likely explanation is that soot-containing particles were measured in the western port regions of the LA Basin onboard the R/V *Atlantis* where fresh shipping and port emissions prevailed as opposed to the more aged emissions sampled onboard the aircraft. Fresh emissions from industrial sources at the port and ocean-going vessels contain high levels of $SO_{2(g)}$ leading to elevated levels of particulate sulfate [*Agrawal et al*., 2008; *Ault et al*., 2010; *Corbett and Fischbeck*, 1997; *Corbett and Koehler*, 2003]. During CalNex, Aged Soot (sulfate) particles were typically found to peak at

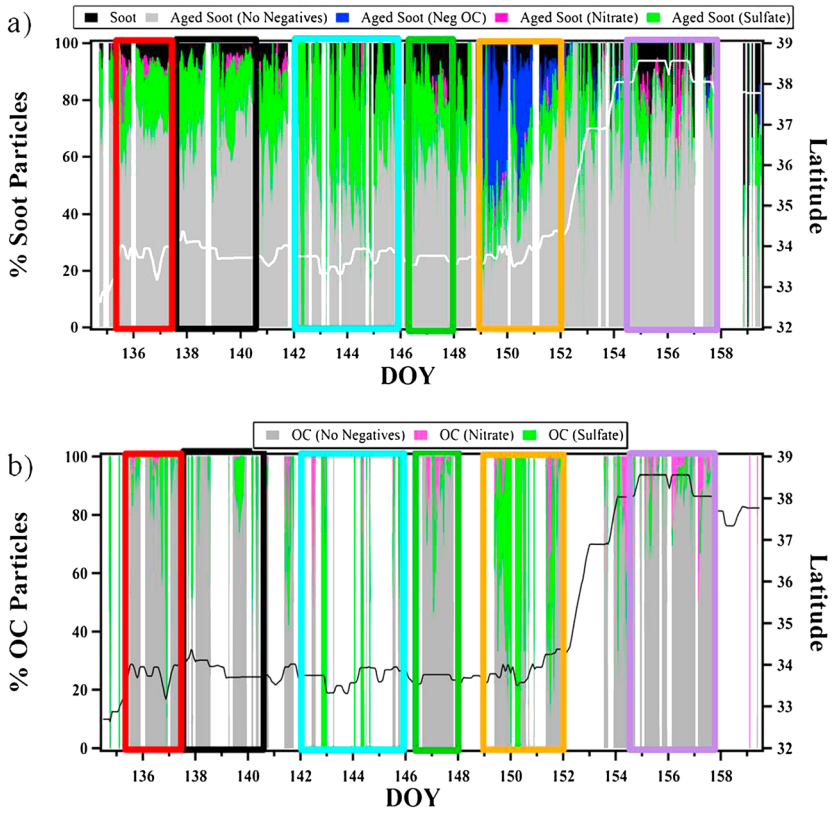

Figure 7. Hourly temporal trends in carbonaceous mixing state. (a) Hourly temporal trends for different soot particle types: Soot (black), Aged Soot (No Negatives) (grey), Aged Soot (Sulfate) (green), Aged Soot (Nitrate) (pink), and Aged Soot (Neg OC) (blue) in addition to latitude (white line). (b) Hourly temporal trends for different organic particle types: OC (No Negatives) (grey), OC (Sulfate) (green), and OC (Nitrate) (pink) in addition to latitude (black line). White spaces denote periods when no OC particles were present. The six different time periods are boxed.

~0.55 μm on average, which is larger than expected for freshly emitted soot particles [*Moffet and Prather*, 2009]; this is likely due to condensation and aqueous phase processing of $SO_{2(g)}$, which has been shown to contribute high quantities of sulfate to particles in this size range in the LA Basin [*Hegg*, 1985; *Hering and Friedlander*, 1982; *Meng and Seinfeld*, 1994]. It should be noted that regulations were adopted in 2009 requiring ships to switch from high-sulfur to low-sulfur fuel within 24 nautical miles of the California coast [*California Air Resources Board*, 2009]. Hence, in addition to fresh port and shipping emissions, another potential source of elevated sulfate on soot particles, particularly during Marine/Coastal Transport conditions (Period 3), is the presence of red tide blooms in Southern Californian waters during CalNex (www.sccoos.org) of *Lingulodinium polyedrum*, a marine organism that has been shown to contribute biogenic sulfur to aerosols [*Gaston et al*., 2010]. Although ATOFMS cannot be used to distinguish biogenic and anthropogenic sulfate, MSA, an ocean-derived biogenic form of sulfur, can be detected and used to assess the possibility of biogenic contributions to detected sulfate levels [*Gaston et al*., 2010]. In fact, ~38% of Aged Soot (sulfate) particles, on average during the Riverside, Stagnant/Ports, Marine, and Ports of LA/LB periods, were found to also contain MSA with the highest percentage (~62% of Aged Soot (sulfate) particles) occurring during the Marine/Coastal Transport period while the lowest percentage (~13% of Aged Soot (sulfate) particles) was observed during the Ports of LA/LB period. This suggests that at least some of the observed sulfate was from a biogenic source.

[23] Agricultural emissions were also found to impact soot mixing state by contributing Aged Soot (nitrate) particles, particularly during the Riverside Transport and Bay Area/Sacramento periods and toward the end of the Stagnant/Ports Transport period, when air masses were transported from the Central Valley. These particles had similar positive ion markers to the Aged Soot (sulfate) particles, but contained nitrate peaks ($^{46}NO_2^-$, $^{62}NO_3^-$) that were more intense than sulfate (see Figure 5f). This particle type has been shown to result from the acquisition of nitrate namely formed through photochemically produced nitric acid ($HNO_{3(g)}$), which condenses onto particles causing them to grow; aqueous phase processing may also contribute to this growth and the acquisition of nitrate [*Moffet and Prather*, 2009; *Moffet et al*., 2008b]. This particle type represented up to ~33% of soot-containing particles and was observed to peak at a larger size mode than the other soot-containing particle types at ~0.75 μm during the campaign (Figure 4).

[24] In addition to Aged Soot (nitrate) particles, unique Aged Soot particles containing sulfate and intense ions at *m/z* −43, −57, and −71 (see Figure 5g) were detected during a period of agricultural influence (Inland/Valley

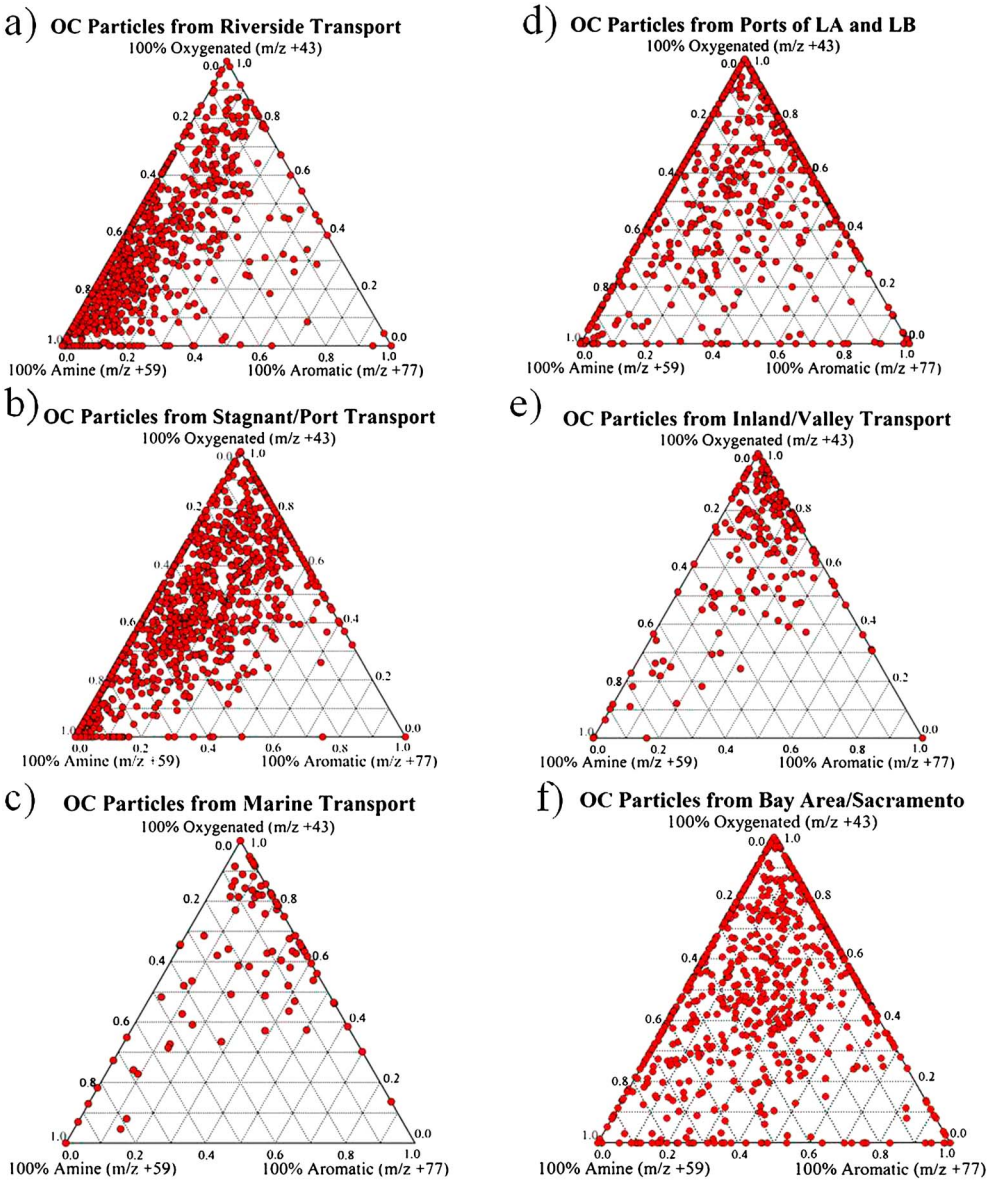

Figure 8. (a–f) Ternary plots for individual OC particles observed for the six different time periods. The top corner of the ternary plots corresponds to OC particles containing only the oxygenated organic peak ($^{43}C_2H_3O^+$), the left bottom corner denotes OC particles containing only the amine peak ($^{59}(CH_3)_3N^+$), and the right bottom corner corresponds to OC particles containing only the aromatic peak ($^{77}C_6H_5^+$).

Transport conditions). To the best of our knowledge, mixtures of soot and these ions have never been detected before by ATOFMS. Since organic peaks in Aged Soot particles typically appear as positive ions, this particle type has been labeled Aged Soot (Neg OC). It is most likely that this particle type is derived from a unique, fresh source near the sampling site, since these ion markers were not observed on other particle types. Further evidence for this speculation comes from the fact that this particle type peaks at a smaller size (~0.35 μm) than the other soot-containing types, as shown in Figure 4e, suggesting a local source. The unique organic markers likely correspond to $^{43}CH_3CO^-$, $^{57}C_2O_2H^-$, and $^{71}C_3H_3O_2^-$ [*McLafferty and Turecek*, 1993; *Silva et al.*, 1999; *Silva and Prather*, 2000] possibly due to contributions from levoglucason and/or methylglyoxal (*m/z* −71), glyoxal (*m/z* −57), and acetaldehyde (*m/z* −43) [*Silva et al.*, 1999; *Silva and Prather*, 2000]. These organic species could represent secondary organic aerosol (SOA) formed from the photolytic processing of organics in the aqueous phase [*Bateman et al.*, 2011]; this mechanism was suggested to contribute organic components with elevated atomic O:C ratios during CalNex [*Duong et al.*, 2011]. Additional field and laboratory measurements are required to confirm the identification of these ion peaks.

3.3.2. The Mixing State of Organic Particles

[25] In addition to soot-containing particles, the mixing state of OC particles (e.g., non-soot-containing OC particles) was also investigated by examining temporal trends. These non-soot-containing OC particles are distinguished from the Aged Soot types described above in that these particles are not characterized by intense elemental carbon peaks at *m/z* +12, +24, +36, etc., but instead have *m/z* +27, +37,

and/or +43 as the main positive ion peaks. Three types of OC particles were identified during CalNex: OC (no negatives), OC (sulfate), and OC (nitrate). Temporal trends of the OC particle types are shown in Figure 7b. Most OC particles were found to lack negative ion spectra (~67 ± 37% on average; see Figure 5h) and peaked in the 0.5–0.6 μm size range (Figure 4) suggesting that they contained appreciable particulate water similar to soot-containing particles. However, during Marine/Coastal and Inland/Valley Transport conditions (Periods 3 and 5), OC particles containing intense sulfate peaks (see Figure 5i) were more common, representing ~55 ± 40% of organic particles on average, likely due to photochemically produced sulfate possibly derived from biogenic emissions. In addition to sulfate, OC particles with intense nitrate peaks (see Figure 5j) were also observed, namely, at night during the Marine/Coastal Transport, Ports of LA/LB, Inland/Valley Transport, and Bay Area/Sacramento periods (Periods 3–6) and represented ~9 ± 17% of organic particles, on average. Overall, OC (nitrate) particles peaked at a smaller particle size (~0.35 μm) suggesting that not all of the nitrate on these particles was due to photochemically produced nitrate, which typically leads to larger particle sizes. Instead, these observations suggest possible contributions of organonitrates formed from reactions with gas-phase precursors and nitrate radical at night that then condense onto particles [*Ng et al*., 2008]; organonitrates were also found to contribute to the organic aerosol burden during CalNex in Bakersfield, CA [*Rollins et al*., 2012].

[26] The OC types described above also frequently contained aromatic peaks ($^{51}C_4H_3^+$, $^{63}C_5H_3^+$, $^{77}C_6H_5^+$, etc.) [*Silva and Prather*, 2000], which have been associated with secondary processing of organic species in vehicle exhaust [*Shields et al*., 2007; *Sodeman et al*., 2005; *Spencer et al*., 2006; *Toner et al*., 2008] and humic substances formed from biomass burning [*Holecek et al*., 2007; *Mayol-Bracero et al*., 2002; *Qin and Prather*, 2006]. OC particles also contained ion peaks indicative of amines (e.g., $^{59}(CH_3)_3N^+$, $^{86}(C_2H_5)_2NCH_2^+$, $^{101}(C_2H_5)_3N^+$, $^{118}(C_2H_5)_3NOH^+$, etc.), which are semivolatile species that can partition onto preexisting particles [*Angelino et al*., 2001; *Pratt et al*., 2009; *Schade and Crutzen*, 1995], and oxidized organic markers (e.g., $^{43}C_2H_3O^+$) that indicate the presence of SOA (see Figure 5h) [*Qin et al*., 2012]. Ternary plots were used to examine the prevalence of these compounds and to further elucidate the mixing state and sources of OC particles using the ion peaks $^{59}(CH_3)_3N^+$, $^{43}C_2H_3O^+$, and $^{77}C_6H_5^+$ as markers for amines, SOA/oxidized organics, and aromatics, respectively (see Figure 8).

[27] Amines were found to dominate the OC mixing state during the first two periods, with 65 ± 33% of OC particles containing intense amine markers during the Riverside Transport period and 48 ± 44% during the Stagnant/Ports Transport period (Figure 8). Dairy farm emissions from the Chino and Central Valley regions in addition to possible contributions from traffic emissions wherein ammonia and amines can be produced from catalytic converters [*Fraser and Cass*, 1998; *Sodeman et al*., 2005], explain the dominance of amines during these two time periods [*Hughes et al*., 2002; *Pastor et al*., 2003; *Pratt et al*., 2009; *Qin et al*., 2012; *Schade and Crutzen*, 1995; *Sorooshian et al*., 2008]. Furthermore, during these two periods, low temperatures and the highest average RH values were measured on the ship; similar meteorological conditions encountered during transport would also favor the detection of amines during these periods [*Angelino et al*., 2001]. Furthermore, 18 ± 23% of OC particles contained intense amine markers during the Ports of LA/LB period even though inland transport conditions were not encountered suggesting that ports could contribute an industrial source of amines, possibly from vehicle emissions including heavy-duty diesel vehicles [*Bishop et al*., 2012; *Fraser and Cass*, 1998; *Sodeman et al*., 2005]. Amines could also have resulted from marine biogenic emissions [*Facchini et al*., 2008a; *Sorooshian et al*., 2009].

[28] Oxidized organics were prevalent during Inland/Valley Transport conditions (Period 5; Figure 8e). The high O_3 concentrations and photochemically aged nature of the sampled air masses suggest that the organics during the Inland/Valley Transport period resulted from secondary rather than primary sources [*Na et al*., 2004; *Qin et al*., 2012]. Oxidized organics at *m/z* +43 were also prevalent during the Stagnant/Ports Transport period, when photochemically aged air masses were sampled, and dominant during Marine/Coastal Transport conditions (Period 3), likely due to secondary contributions. Another source of the oxidized organics during the Marine/Coastal Transport period could be organics from marine biogenic sources, such as lipopolysaccharides, that have higher oxygen content than organics from anthropogenic sources [*Facchini et al*., 2008b; *Ovadnevaite et al*., 2011; *Russell et al*., 2011; *Russell et al*., 2010].

[29] SOA from aromatics was more prevalent during the Ports of LA/LB and Bay Area/Sacramento periods than during any other periods; however, oxidized organics were still the most prevalent type of organics during these two periods. The increased frequency of aromatic markers in the Ports of LA and LB is likely due to increased emissions from diesel combustion by trucks [*Kasper et al*., 2007; *Maricq*, 2007; *Shields et al*., 2007; *Spencer et al*., 2006] in addition to emissions from ships [*Kasper et al*., 2007; *Lack et al*., 2009; *Murphy et al*., 2009; *Russell et al*., 2009]. Oxidized organics and amines in Sacramento are likely from agricultural and biogenic emissions [*Chow et al*., 2006b; *Setyan et al*., 2012; *Sorooshian et al*., 2008] while the observed SOA from aromatics are likely humic substances derived from biomass burning [*Holecek et al*., 2007; *Mayol-Bracero et al*., 2002].

4. Conclusions and Implications for California

[30] Overall, we found that the chemical properties of aerosol particles differed widely across California based on particle source and transport conditions. As evidenced by the particle chemistry and mixing state measured onboard the R/V *Atlantis*, Southern California was impacted by fresh shipping and vehicular emissions from cars and diesel trucks in addition to marine biogenic emissions. Soot-containing particles were the most prevalent submicron particles in Southern California and were typically mixed with sulfate while aromatic markers were found to contribute to organics due to residual fuel, distillate fuel, and gasoline combustion. These fresh emissions were episodically mixed with inland, agricultural emissions leading to the presence of secondary

species such as amines. It is important to note that the particles measured in Southern California contained elevated levels of sulfate because these measurements focused on fresh emissions from the Ports of LA and LB; if these measurements were made farther inland of the ports, enhancements in nitrate namely due to particle aging and contributions of ammonium nitrate, as seen by other measurements, would have been observed instead [*Cahill et al*., 2012; *Metcalf et al*., 2012].

[31] In contrast, Northern California was impacted by biogenic emissions from the forested Sierra Nevada foothills and agricultural emissions as evidenced by the prevalence of organic carbon [*Cahill et al*., 2012; *Setyan et al*., 2012]. Oxidized organic compounds were frequently associated with particles during Inland/Valley transport conditions and in Sacramento, likely due to contributions from SOA while aromatic markers observed in Sacramento are likely due to contributions from biomass burning.

[32] Overall, we found that the mixing state of particles in California varies significantly on a regional scale due to diverse local sources. Furthermore, the mixing state of particles from these local emissions can be significantly altered based on differences in meteorological conditions and air mass histories, which will most likely result in regional differences in the health, optical, and cloud-nucleating properties for the aerosol populations observed across California. This should be taken into account when determining which emissions sources to regulate in order to mitigate the adverse effects of aerosols on both human health and climate change.

[33] **Acknowledgments.** The authors would like to thank Derek Coffman, Drew Hamilton, and the entire crew of the R/V *Atlantis* for assistance during the CalNex field campaign. Chris Cappa is acknowledged for assistance with filtering out ship exhaust time periods. Dan Cziczo is acknowledged for assistance prior to the CalNex campaign. We gratefully acknowledge the NOAA Air Resources Laboratory for the provision of the HYSPLIT transport model and READY website (http://ready.arl.noaa.gov/HYSPLIT.php) used in this publication. The authors also gratefully acknowledge the Southern California Coastal Ocean Observing System (SCCOOS) (www.sccoos.org/) for the provision of harmful algal bloom data used in this publication. Eric J. Williams and Brian Lerner are acknowledged for use of NO_x and NO_y data onboard the R/V *Atlantis*. The entire Prather group is acknowledged for helpful comments and discussion. The authors would like to thank anonymous reviewers for their suggestions and comments. C.J.G. was funded through the Aerosol Chemistry and Climate Institute at Pacific Northwest National Laboratory. This work was funded by the California Air Resources Board (CARB).

References

Agrawal, H., Q. G. J. Malloy, W. A. Welch, J. W. Miller, and D. R. Cocker (2008), In-use gaseous and particulate matter emissions from a modern ocean going container vessel, *Atmos. Environ.*, *42* (21), 5504–5510.

Ahlm, L., et al. (2012), Formation and growth of ultrafine particles from secondary sources in Bakersfield, California, *J. Geophys. Res.*, *117*, D00V08, doi:10.1029/2011JD017144.

Allen, J. O. (2002), YAADA software toolkit to analyze single-particle mass spectral data: Reference manual version 1.1, *Arizona State University*, http://www.yaada.org.

Angelino, S., D. T. Suess, and K. A. Prather (2001), Formation of aerosol particles from reactions of secondary and tertiary alkylamines: Characterization by aerosol time-of-flight mass spectrometry, *Environ. Sci. Tech.*, *35*(15), 3130–3138.

Ault, A. P., M. J. Moore, H. Furutani, and K. A. Prather (2009), Impact of emissions from the Los Angeles port region on San Diego air quality during regional transport events, *Environ. Sci. Tech.*, *43*(10), 3500–3506.

Ault, A. P., C. J. Gaston, Y. Wang, G. Dominguez, M. H. Thiemens, and K. A. Prather (2010), Characterization of the single particle mixing state of individual ship plume events measured at the Port of Los Angeles, *Environ. Sci. Tech.*, *44*(6), 1954–1961.

Bateman, A. P., S. A. Nizkorodov, J. Laskin, and A. Laskin (2011), Photolytic processing of secondary organic aerosols dissolved in cloud droplets, *Phys. Chem. Chem. Phys.*, *13*, 12,199–12,212.

Bates, T. S., et al. (2004), Marine boundary layer dust and pollutant transport associated with the passage of a frontal system over eastern Asia, *J. Geophys. Res.*, *109*, D19S19, doi:10.1029/2003JD004094.

Bates, T. S., et al. (2012), Measurements of ocean derived aerosol off the coast of California, *J. Geophys. Res.*, *117*, D00V15, doi:10.1029/2012JD017588.

Behnke, W., H. U. Kruger, V. Scheer, and C. Zetzsch (1991), Formation of atomic Cl from sea spray via photolysis of nitryl chloride—Determination of the sticking coefficient of N_2O_5 on NaCl aerosol, *J. Aerosol Sci.*, *22*, S609–S612.

Bishop, G. A., B. G. Schuchmann, and D. H. Stedman (2012), Emission changes resulting from the San Pedro Bay, California ports truck retirement program, *Environ. Sci. Tech.*, *46*, 551–558.

Blanchard, D. C., and A. H. Woodcock (1957), Bubble formation and modification in the sea and its meteorological significance, *Tellus*, *9*(2), 145–158.

Bon, D. M., et al. (2011), Measurements of volatile organic compounds at a suburban ground site (T1) in Mexico City during the MILAGRO 2006 campaign: Measurement comparison, emission ratios, and source attribution, *Atmos. Chem. Phys.*, *11*, 2399–2421.

Cahill, J. F., K. Suski, J. Seinfeld, R. A. Zaveri, and K. A. Prather (2012), The mixing state between northern and southern California measured during CARES and CalNEX 2010, *Atmos. Chem. Phys.*, *12*, 10,989–11,002, doi:10.5194/acp-12-10989-2012.

California Air Resources Board (2009), *Final Regulation Order. Fuel Sulfur and Other Operational Requirements for Ocean-Going Vessels within California Waters and 24 Nautical Miles of the California Baseline*, California Air Resources Board, Sacramento, CA.

Chang, W. L., P. V. Bhave, S. S. Brown, N. Riemer, J. Stutz, and D. Dabdub (2011), Heterogeneous atmospheric chemistry, ambient measurements, and model calculations of N_2O_5: A review, *Aerosol Sci. Tech.*, *45*(6), 665–695.

Chen, L. W. A., J. G. Watson, J. C. Chow, and K. L. Magliano (2007), Quantifying $PM_{2.5}$ source contributions for the San Joaquin Valley with multivariate receptor models, *Environ. Sci. Tech.*, *41*(8), 2818–2826.

Chow, J. C., L. W. A. Chen, J. G. Watson, D. H. Lowenthal, K. A. Magliano, K. Turkiewicz, and D. E. Lehrman (2006a), $PM_{2.5}$ chemical composition and spatiotemporal variability during the California Regional PM_{10}/$PM_{2.5}$ Air Quality Study (CRPAQS), *J. Geophys. Res.*, *111*, D10S04, doi:10.1029/2005JD006457.

Chow, J. C., J. G. Watson, D. H. Lowenthal, L. W. A. Chen, and K. L. Magliano (2006b), Particulate carbon measurements in California's San Joaquin Valley, *Chemosphere*, *62*(3), 337–348.

Corbett, J. J., and P. Fischbeck (1997), Emissions from ships, *Science*, *278*(5339), 823–824.

Corbett, J. J., and H. W. Koehler (2003), Updated emissions from ocean shipping, *J. Geophys. Res.*, *108*(D20), 4650, doi:10.1029/2003JD003751.

Creamean, J. M., A. P. Ault, J. E. Ten Hoeve, M. Z. Jacobson, G. C. Roberts, and K. A. Prather (2011), Measurements of aerosol chemistry during new particle formation events at a remote rural mountain site, *Environ. Sci. Tech.*, *45*(19), 8208–8216.

Dall'Osto, M., R. M. Harrison, D. C. S. Beddows, E. J. Freney, M. R. Heal, and R. J. Donovan (2006), Single-particle detection efficiencies of aerosol time-of-flight mass spectrometry during the North Atlantic marine boundary layer experiment, *Environ. Sci. Tech.*, *40*(16), 5029–5035.

Docherty, K. S., et al. (2008), Apportionment of primary and secondary organic aerosols in Southern California during the 2005 Study of Organic Aerosols in Riverside (SOAR-1), *Environ. Sci. Tech.*, *42*(20), 7655–7662.

Draxler, R. R., and G. D. Rolph (2011), HYSPLIT (Hybrid Single-Particle Lagrangian Integrated Trajectory) Model access via NOAA ARL READY website (http://ready.arl.noaa.gov/HYSPLIT.php), *NOAA Air Resources Laboratory*, Silver Spring, MD.

Duong, H. T., A. Sorooshian, J. S. Craven, S. P. Hersey, A. R. Metcalf, X. Zhang, R. J. Weber, H. H. Jonsson, R. C. Flagan, and J. H. Seinfeld (2011), Water-soluble organic aerosol in the Los Angeles Basin and outflow regions: Airborne and ground measurements during the 2010 CalNex field campaign, *J. Geophys. Res.*, *116*, D00V04, doi:10.1029/2011JD016674.

Eatough, D. J., B. D. Grover, W. R. Woolwine, N. L. Eatough, R. Long, and R. Farber (2008), Source apportionment of 1 h semi-continuous data during the 2005 Study of Organic Aerosols in Riverside (SOAR) using positive matrix factorization, *Atmos. Environ.*, *42*(11), 2706–2719.

Facchini, M. C., et al. (2008a), Important source of marine secondary organic aerosol from biogenic amines, *Environ. Sci. Tech.*, *42*(24), 9116–9121.

Facchini, M. C., et al. (2008b), Primary submicron marine aerosol dominated by insoluble organic colloids and aggregates, *Geophys. Res. Lett.*, *35*, L17814, doi:10.1029/2008GL034210.

Fitzgerald, J. W. (1991), Marine aerosols: A review, *Atmos. Environ. A-Gen. Topics*, *25*(3–4), 533–545.

Fraser, M. P., and G. R. Cass (1998), Detection of excess ammonia emissions from in-use vehicles and the implications for fine particle control, *Environ. Sci. Tech.*, *32*, 1053–1057.

Gard, E., J. E. Mayer, B. D. Morrical, T. Dienes, D. P. Fergenson, and K. A. Prather (1997), Real-time analysis of individual atmospheric aerosol particles: Design and performance of a portable ATOFMS, *Anal. Chem.*, *69*(20), 4083–4091.

Gard, E. E., et al. (1998), Direct observation of heterogeneous chemistry in the atmosphere, *Science*, *279*(5354), 1184–1187.

Gaston, C. J., K. A. Pratt, X. Y. Qin, and K. A. Prather (2010), Real-time detection and mixing state of methanesulfonate in single particles at an inland urban location during a phytoplankton bloom, *Environ. Sci. Tech.*, *44*(5), 1566–1572.

Gaston, C. J., H. Furutani, S. A. Guazzotti, K. R. Coffee, T. S. Bates, P. K. Quinn, L. I. Aluwihare, B. G. Mitchell, and K. A. Prather (2011), Unique ocean-derived particles serve as a proxy for changes in ocean chemistry, *J. Geophys. Res.*, *116*, D18310, doi:10.1029/2010JD015289.

Gelencser, A., K. Siszler, and J. Hlavay (1997), Toluene-benzene concentration ratio as a tool for characterizing the distance from vehicular emission sources, *Environ. Sci. Tech.*, *31*, 2869–2872.

Grover, B. D., N. L. Eatough, W. R. Woolwine, J. P. Cannon, D. J. Eatough, and R. W. Long (2008), Semi-continuous mass closure of the major components of fine particulate matter in Riverside, CA, *Atmos. Environ.*, *42*, 250–260.

Guazzotti, S. A., K. R. Coffee, and K. A. Prather (2001), Continuous measurements of size-resolved particle chemistry during INDOEX-Intensive Field Phase 99, *J. Geophys. Res.*, *106*(D22), 28,607–28,627.

Hawkins, L. N., L. M. Russell, D. S. Covert, P. K. Quinn, and T. S. Bates (2010), Carboxylic acids, sulfates, and organosulfates in processed continental organic aerosol over the southeast Pacific Ocean during VOCALS-REx 2008, *J. Geophys. Res.*, *115*, D13201, doi:10.1029/2009JD013276.

Healy, R. M., I. P. O'Connor, S. Hellebust, A. Allanic, J. R. Sodeau, and J. C. Wenger (2009), Characterization of single particles from in-port ship emissions, *Atmos. Environ.*, *43*, 6408–6414.

Hegg, D. A. (1985), The importance of liquid-phase oxidation of SO_2 in the troposphere, *J. Geophys. Res.*, *90*(D2), 3773–3779.

Hegg, D. A., and M. B. Baker (2009), Nucleation in the atmosphere, *Rep. Prog. Phys.*, *72*(5), doi:10.1088/0034-4885/72/5/056801.

Hering, S. V., and S. K. Friedlander (1982), Origins of aerosol sulfur size distributions in the Los Angeles Basin, *Atmos. Environ.*, *16*(11), 2647–2656.

Holecek, J. C., M. T. Spencer, and K. A. Prather (2007), Analysis of rainwater samples: Comparison of single particle residues with ambient particle chemistry from the northeast Pacific and Indian oceans, *J. Geophys. Res.*, *112*, D22S24, doi:10.1029/2006JD008269.

Hopkins, R. J., Y. Desyaterik, A. V. Tivanski, R. A. Zaveri, C. M. Berkowitz, T. Tyliszczak, M. K. Gilles, and A. Laskin (2008), Chemical speciation of sulfur in marine cloud droplets and particles: Analysis of individual particles from the marine boundary layer over the California Current, *J. Geophys. Res.*, *113*, D04209, doi:10.1029/2007JD008954.

Hughes, L. S., J. O. Allen, P. Bhave, M. J. Kleeman, G. R. Cass, D. Y. Liu, D. F. Fergenson, B. D. Morrical, and K. A. Prather (2000), Evolution of atmospheric particles along trajectories crossing the Los Angeles basin, *Environ. Sci. Tech.*, *34*(15), 3058–3068.

Hughes, L. S., J. O. Allen, L. G. Salmon, P. R. Mayo, R. J. Johnson, and G. R. Cass (2002), Evolution of nitrogen species air pollutants along trajectories crossing the Los Angeles area, *Environ. Sci. Tech.*, *36*(18), 3928–3935.

Kasper, A., S. Aufdenblatten, A. Forss, M. Mohr, and H. Burtscher (2007), Particulate emissions from a low-speed marine diesel engine, *Aerosol Sci. Tech.*, *41*(1), 24–32.

Kulmala, M. (2003), How particles nucleate and grow, *Science*, *302*(5647), 1000–1001.

Lack, D. A., et al. (2009), Particulate emissions from commercial shipping: Chemical, physical, and optical properties, *J. Geophys. Res.*, *114*, D00F04, doi:10.1029/2008JD011300.

Laskin, A., R. C. Moffet, M. K. Gilles, J. D. Fast, R. A. Zaveri, B. Wang, P. Nigge, and J. Shutthanandan (2012), Tropospheric chemistry of internally mixed sea salt and organic particles: Surprising reactivity of NaCl with weak organic acids, *J. Geophys. Res.*, *117*, D15302, doi:10.1029/2012JD017743.

Liu, D.-Y., K. A. Prather, and S. V. Herring (2000), Variations in the size and chemical composition of nitrate-containing particles in Riverside, CA, *Aerosol Sci. Tech.*, *33*(1–2), 71–86.

Magliano, K. L., V. M. Hughes, L. R. Chinkin, D. L. Coe, T. L. Haste, N. Kumar, and F. W. Lurmann (1999), Spatial and temporal variations in PM_{10} and $PM_{2.5}$ source contributions and comparison to emissions during the 1995 integrated monitoring study, *Atmos. Environ.*, *33*(29), 4757–4773.

Maricq, M. M. (2007), Chemical characterization of particulate emissions from diesel engines: A review, *J. Aerosol Sci.*, *38*(11), 1079–1118.

Mayol-Bracero, O. L., P. Guyon, B. Graham, G. Roberts, M. O. Andreae, S. Decesari, M. C. Facchini, S. Fuzzi, and P. Artaxo (2002), Water-soluble organic compounds in biomass burning aerosols over Amazonia—2. Apportionment of the chemical composition and importance of the polyacidic fraction, *J. Geophys. Res.*, *107*(D20), 8091, doi:10.1029/2001JD000522.

McLafferty, F. W., and F. Turecek (1993), *Interpretation of Mass Spectra*, University Science Books, Sausalito, CA.

Meng, Z., and J. H. Seinfeld (1994), On the source of the submicrometer droplet mode of urban and regional aerosols, *Aerosol Sci. Tech.*, *20*, 253–265.

Metcalf, A. R., J. S. Craven, J. J. Ensberg, J. Brioude, W. Angevine, A. Sorooshian, H. T. Duong, H. H. Jonsson, R. C. Flagan, and J. H. Seinfeld (2012), Black carbon aerosol over the Los Angeles Basin during CalNex, *J. Geophys. Res.*, *117*, D00V13, doi:10.1029/2011JD017255.

Moffet, R. C., and K. A. Prather (2009), In-situ measurements of the mixing state and optical properties of soot with implications for radiative forcing estimates, *P. Natl. Acad. Sci.*, *106*(29), 11872–11877.

Moffet, R. C., et al. (2008a), Characterization of aerosols containing Zn, Pb, and Cl from an industrial region of Mexico City, *Environ. Sci. Tech.*, *42*(19), 7091–7097.

Moffet, R. C., X. Qin, T. Rebotier, H. Furutani, and K. A. Prather (2008b), Chemically segregated optical and microphysical properties of ambient aerosols measured in a single-particle mass spectrometer, *J. Geophys. Res.*, *113*, D12213, doi:10.1029/2007JD009393.

Monahan, E. C., C. W. Fairall, K. L. Davidson, and P. J. Boyle (1983), Observed interrelations between 10 m winds, ocean whitecaps and marine aerosols, *Q. J. R. Meteorolog. Soc.*, *109*(460), 379–392.

Murphy, S. M. A., et al. (2009), Comprehensive simultaneous shipboard and airborne characterization of exhaust from a modern container ship at sea, *Environ. Sci. Tech.*, *43*(13), 4626–4640.

Na, K., A. A. Sawant, C. Song, and D. R. Cocker (2004), Primary and secondary carbonaceous species in the atmosphere of Western Riverside County, California, *Atmos. Environ.*, *38*, 1345–1355.

Neubauer, K. R., M. V. Johnston, and A. S. Wexler (1997), On-line analysis of aqueous aerosols by laser desorption ionization, *Int. J. Mass Spectrom. Ion Processes*, *163*(1–2), 29–37.

Neubauer, K. R., M. V. Johnston, and A. S. Wexler (1998), Humidity effects on the mass spectra of single aerosol particles, *Atmos. Environ.*, *32*(14–15), 2521–2529.

Ng, N. L., et al. (2008), Secondary organic aerosol (SOA) formation from reaction of isoprene with nitrate radicals (NO_3), *Atmos. Chem. Phys.*, *8*(14), 4117–4140.

Nguyen, T. B., P. J. Roach, J. Laskin, A. Laskin, and S. A. Nizkorodov (2011), Effect of humidity on the composition of isoprene photooxidation secondary organic aerosol, *Atmos. Chem. Phys.*, *11*, 6931–6944.

Noble, C. A., and K. A. Prather (1996), Real-time measurement of correlated size and composition profiles of individual atmospheric aerosol particles, *Environ. Sci. Tech.*, *30*(9), 2667–2680.

O'Dowd, C. D., and G. De Leeuw (2007), Marine aerosol production: A review of the current knowledge, *Phil. Trans. A*, *365*(1856), 1753–1774.

Ovadnevaite, J., C. O'Dowd, M. Dall'Osto, D. Ceburnis, D. R. Worsnop, and H. Berresheim (2011), Detecting high contributions of primary organic matter to marine aerosol: A case study, *Geophys. Res. Lett.*, *38*, L02807, doi:10.1029/2010GL046083.

Pastor, S. H., J. O. Allen, L. S. Hughes, P. Bhave, G. R. Cass, and K. A. Prather (2003), Ambient single particle analysis in Riverside, California by aerosol time-of-flight mass spectrometry during the SCOS97-NARSTO, *Atmos. Environ.*, *37*, S239–S258.

Poschl, U. (2005), Atmospheric aerosols: Composition, transformation, climate and health effects, *Angew. Chem. Int. Ed.*, *44*(46), 7520–7540.

Prather, K. A., T. Nordmeyer, and K. Salt (1994), Real-time characterization of individual aerosol-particles using time-of-flight mass-spectrometry, *Anal. Chem.*, *66*(9), 1403–1407.

Pratt, K. A., and K. A. Prather (2009), Real-time, single-particle volatility, size, and chemical composition measurements of aged urban aerosols, *Environ. Sci. Tech.*, *43*(21), 8276–8282.

Pratt, K. A., and K. A. Prather (2011), Mass spectrometry of atmospheric aerosols—Recent developments and applications. Part II: On-line mass spectrometry techniques, *Mass Spectrom. Rev.*, *31*, 17–48, doi:10.1002/mas.20330.

Pratt, K. A., L. E. Hatch, and K. A. Prather (2009), Seasonal volatility dependence of ambient particle phase amines, *Environ. Sci. Tech.*, *43*(14), 5276–5281.

Pratt, K. A., A. J. Heymsfield, C. H. Twohy, S. M. Murphy, P. J. DeMott, J. G. Hudson, R. Subramanian, Z. E. Wang, J. H. Seinfeld, and K. A. Prather (2010), In situ chemical characterization of aged biomass-burning aerosols impacting cold wave clouds, *J. Atmos. Sci.*, *67*(8), 2451–2468.

Qin, X. Y., and K. A. Prather (2006), Impact of biomass emissions on particle chemistry during the California Regional Particulate Air Quality Study, *Int. J. Mass Spectrom.*, *258*(1–3), 142–150.

Qin, X. Y., P. V. Bhave, and K. A. Prather (2006), Comparison of two methods for obtaining quantitative mass concentrations from aerosol time-of-flight mass spectrometry measurements, *Anal. Chem.*, *78*(17), 6169–6178.

Qin, X., K. A. Pratt, L. G. Shields, S. M. Toner, and K. A. Prather (2012), Seasonal comparisons of single-particle chemical mixing state in Riverside, CA, *Atmos. Environ.*, *59*, 587–596.

Quinn, P. K., and T. S. Bates (2005), Regional aerosol properties: Comparisons of boundary layer measurements from ACE 1, ACE 2, Aerosols99, INDOEX, ACE Asia, TARFOX, and NEAQS, *J. Geophys. Res.*, *110*, D14202, doi:10.1029/2004JD004755.

Roberts, J. M., F. C. Fehsenfeld, S. C. Liu, M. J. Bollinger, C. Hahn, D. L. Albritton, and R. E. Sievers (1984), Measurements of aromatic hydrocarbon ratios and NO_x concentrations in the rural troposphere: Observation of air mass photochemical aging and NO_x removal, *Atmos. Environ.*, *18* (11), 2421–2432.

Rollins, A. W., et al. (2012), Evidence for NO_x control over nighttime SOA formation, *Science*, *337*(6099), 1210–1212.

Russell, L. M., K. J. Noone, R. J. Ferek, R. A. Pockalny, R. C. Flagan, and J. H. Seinfeld (2000), Combustion organic aerosol as cloud condensation nuclei in ship tracks, *Am. Meteorol. Soc.*, 2591–2606.

Russell, L. M., S. Takahama, S. Liu, L. N. Hawkins, D. S. Covert, P. K. Quinn, and T. S. Bates (2009), Oxygenated fraction and mass of organic aerosol from direct emission and atmospheric processing measured on the R/V *Ronald Brown* during TEXAQS/GoMACCS 2006, *J. Geophys. Res.*, *114*, D00F05, doi:10.1029/2008JD011275.

Russell, L. M., L. N. Hawkins, A. A. Frossard, P. K. Quinn, and T. S. Bates (2010), Carbohydrate-like composition of submicron atmospheric particles and their production from ocean bubble bursting, *P. Natl. Acad. Sci.*, *107*(15), 6652–6657.

Russell, L. M., R. Bahadur, and P. J. Ziemann (2011), Identifying organic aerosol sources by comparing functional group composition in chamber and atmospheric particles, *P. Natl. Acad. Sci.*, doi:10.1073/pnas.1006461108.

Ryerson, T. B., et al. (2013), The 2010 California Research at the Nexus of Air Quality and Climate Change (CalNex) field study, *J. Geophys. Res.*, doi:10.1002/jgrd.50331, In Press.

Schade, G. W., and P. J. Crutzen (1995), Emission of aliphatic amines from animal husbandry and their reactions: Potential source of N_2O and HCN, *J. Atmos. Chem.*, *22*(3), 319–346.

Setyan, A., et al. (2012), Characterization of submicron particles influenced by mixed biogenic and anthropogenic using high-resolution aerosol mass spectrometry: Results from CARES, *Atmos. Chem. Phys.*, *12*, 8131–8156.

Shields, L. G., D. T. Suess, and K. A. Prather (2007), Determination of single particle mass spectral signatures from heavy-duty diesel vehicle emissions for $PM_{2.5}$ source apportionment, *Atmos. Environ.*, *41*(18), 3841–3852.

Silva, P. J., and K. A. Prather (2000), Interpretation of mass spectra from organic compounds in aerosol time-of-flight mass spectrometry, *Anal. Chem.*, *72*(15), 3553–3562.

Silva, P. J., D. Y. Liu, C. A. Noble, and K. A. Prather (1999), Size and chemical characterization of individual particles resulting from biomass burning of local Southern California species, *Environ. Sci. Tech.*, *33*(18), 3068–3076.

Smith, J. N., M. J. Dunn, T. M. VanReken, K. Iida, M. R. Stolzenburg, P. H. McMurry, and L. G. Huey (2008), Chemical composition of atmospheric nanoparticles formed from nucleation in Tecamac, Mexico: Evidence for an important role for organic species in nanoparticle growth, *Geophys. Res. Lett.*, *35*, L04808, doi:10.1029/2007GL032523.

Sodeman, D. A., S. M. Toner, and K. A. Prather (2005), Determination of single particle mass spectral signatures from light-duty vehicle emissions, *Environ. Sci. Tech.*, *39*(12), 4569–4580.

Song, X. H., P. K. Hopke, D. P. Fergenson, and K. A. Prather (1999), Classification of single particles analyzed by ATOFMS using an artificial neural network, ART-2a, *Anal. Chem.*, *71*(4), 860–865.

Sorooshian, A., S. N. Murphy, S. Hersey, H. Gates, L. T. Padro, A. Nenes, F. J. Brechtel, H. Jonsson, R. C. Flagan, and J. H. Seinfeld (2008), Comprehensive airborne characterization of aerosol from a major bovine source, *Atmos. Chem. Phys.*, *8*(17), 5489–5520.

Sorooshian, A., et al. (2009), On the link between ocean biota emissions, aerosol, and maritime clouds: Airborne, ground, and satellite measurements off the coast of California, *Global Biogeochem. Cycles*, *23*, GB4007, doi:10.1029/2009GB003464.

Spencer, M. T., L. G. Shields, D. A. Sodeman, S. M. Toner, and K. A. Prather (2006), Comparison of oil and fuel particle chemical signatures with particle emissions from heavy and light duty vehicles, *Atmos. Environ.*, *40*(27), 5224–5235.

Srivastava, A., et al. (2005), Comprehensive assignment of mass spectral signatures from individual *Bacillus atrophaeus* spores in matrix-free laser desorption/ionization bioaerosol mass spectrometry, *Anal. Chem.*, *77*(10), 3315–3323.

Sullivan, R. C., and K. A. Prather (2005), Recent advances in our understanding of atmospheric chemistry and climate made possible by on-line aerosol analysis instrumentation, *Anal. Chem.*, *77*(12), 3861–3885.

Toner, S. M., L. G. Shields, D. A. Sodeman, and K. A. Prather (2008), Using mass spectral source signatures to apportion exhaust particles from gasoline and diesel powered vehicles in a freeway study using UF-ATOFMS, *Atmos. Environ.*, *42*(3), 568–581.

Twohy, C. H., M. D. Petters, J. R. Snider, B. Stevens, W. Tahnk, M. Wetzel, L. Russell, and F. Burnet (2005), Evaluation of the aerosol indirect effect in marine stratocumulus clouds: Droplet number, size, liquid water path, and radiative impact, *J. Geophys. Res.*, *110*, D08203, doi:10.1029/2004JD005116.

Vogt, R., P. J. Crutzen, and R. Sander (1996), A mechanism for halogen release from sea-salt aerosol in the remote marine boundary layer, *Nature*, *383*(6598), 327–330.

Weiss-Penzias, P., E. Williams, B. Lerner, T. Bates, C. Gaston, K. Prather, A. Vlasenko, and S.-M. Li (2013), Shipboard measurements of gaseous elemental mercury along the coast of Central and Southern California, *J. Geophys. Res.*, *118*, doi:10.1029/2012JD018463.

Wenzel, R. J., D. Y. Liu, E. S. Edgerton, and K. A. Prather (2003), Aerosol time-of-flight mass spectrometry during the Atlanta Supersite Experiment: 2. Scaling procedures, *J. Geophys. Res.*, *108*(D7), 8427,doi:10.1029/2001JD001563.

Whiteaker, J. R., D. T. Suess, and K. A. Prather (2002), Effects of meteorological conditions on aerosol composition and mixing state in Bakersfield, CA, *Environ. Sci. Tech.*, *36*(11), 2345–2353.

Zhang, Q., C. O. Stanier, M. R. Canagaratna, J. T. Jayne, D. R. Worsnop, S. N. Pandis, and J. L. Jimenez (2004), Insights into the chemistry of new particle formation and growth events in Pittsburgh based on aerosol mass spectrometry, *Environ. Sci. Tech.*, *38*(18), 4797–4809.